

# Crystallization Kinetics in Mixtures of Poly( $\epsilon$ -caprolactone) and Poly(styrene-*co*-acrylonitrile)

Zhigang Wang\* and Bingzheng Jiang

Laboratory of Polymer Physics, Changchun Institute of Applied Chemistry,  
Chinese Academy of Sciences, Changchun 130022, P. R. China

Received October 1, 1996; Revised Manuscript Received June 12, 1997

**ABSTRACT:** Isothermal crystallization kinetics in the miscible mixtures of poly( $\epsilon$ -caprolactone) (PCL) and poly(styrene-*co*-acrylonitrile) (SAN) have been investigated as a function of the composition and the crystallization temperature by optical microscopy. The radial growth rates of the spherulites have been described by a kinetic equation including the interaction parameter and the free energy for the formation of secondary crystal nuclei. Fold surface free energies decrease slightly with the increase of SAN content. The experimental findings show that the influence of the glass transition temperature of the mixture, which is related to the chain mobility, on the rate of crystallization predominates over the influence of the surface free energies. This indicates that the glass transition temperature of the mixture should be of more importance, so that the growth rates decrease when the content of the noncrystallizable component increases. In addition, the Flory–Huggins interaction parameter obtained by fitting the kinetic equation with experimental data is questionable.

## Introduction

There are numerous reports on studies of crystallization kinetics in homopolymers, as determined from measurements of spherulitic growth rates.<sup>1–5</sup> The theoretical framework for such studies was originally developed by Turnbull and Fisher in 1949,<sup>6</sup> and subsequently reformulated in molecular terms by Hoffman and co-workers.<sup>2,7–13</sup> The latter treatment is usually referred to as the Lauritzen–Hoffman theory. Spherulitic growth kinetics in miscible blends of noncrystalline and crystalline polymers has also been reported in the past.<sup>14–21</sup> All the previous reports have indicated a depression in growth kinetics of the crystallizable component upon addition of the noncrystallizable component. This depression in kinetics has been attributed to such factors as a reduction in chain mobility due to an increase of the glass transition temperature  $T_g$ , dilution of the crystallizable component at the growth front, changes in free energy of nucleation due to specific interactions, and competition between the advancing spherulitic front and diffusion of the noncrystallizable component into interlamellar and interfibrillar regions. In this study, the spherulitic growth rates of poly( $\epsilon$ -caprolactone) (PCL) in its miscible blends with poly(styrene-*co*-acrylonitrile) (SAN) are reported.

PCL is miscible with SAN on a molecular level within a miscibility window ranging from a copolymer content of 8 to 28 wt % acrylonitrile in SAN.<sup>22</sup> Inside the miscibility window, a one-phase system is formed above the melting point  $T_m$  and below  $T_m$  a neat crystalline PCL phase and a homogeneous, amorphous mixture of PCL and SAN exist. The phase behaviors and resulting morphologies in these blends have been investigated.<sup>23–27</sup> However, limited results on the crystallization kinetics of PCL/SAN blends have been reported.<sup>28–29</sup> Special emphasis has been placed on the Flory–Huggins interaction parameter between the polymers on the growth rates of the PCL spherulites in the mixtures.<sup>30</sup>

In this paper, the influences of several factors on the depression in growth kinetics are discussed. The factors include a reduction in chain mobility due to an increase

of the glass transition temperature  $T_g$ , dilution of the crystallizable component at the growth front, and changes in free surface energy of nucleation due to specific interactions.

## Experimental Section

The PCL specimen was bought from Polysciences Inc. The  $M_w$  and  $M_n$  determined by gel permeation chromatography (gpc) are 22 000 and 11 300, respectively. Their ratio  $\alpha$  is 1.93. The melting temperature of PCL is about 60 °C. The SAN with 25% AN content was supplied by Polysciences Inc., too. The  $M_w$  and  $M_n$  are 197 000 and 106 000 by gpc, and their ratio  $\alpha$  is 1.86. The  $T_g$  of SAN is 105 °C measured by DSC. The samples of PCL/SAN blends with compositions of 100/0, 90/10, 80/20, and 70/30 were prepared by mixing them in  $\text{CH}_2\text{-Cl}_2$ . A dilute solution (5% wt/wt) was stirred continuously for 24 h at 25 °C. Films were obtained by casting four drops of the dilute solution on a clean cover glass and held in a vacuum oven at 40 °C for 3 days.

A polarizing optical microscope (XPT-7, made in Nanjing Jianan Optical Electronic Co. Ltd.) equipped with a MINTRON CCD camera (MTV 1881EX, made in Taiwan) was used to observe the isothermal crystallization process of PCL/SAN blends. Two homemade microscope hot stages were used, with temperatures controlled within  $\pm 0.1$  °C. The films with a free surface upward were first melted on one hot stage at 80 °C for 5 h and then were rapidly transported to another hot stage controlled at the crystallization temperature ( $T_c$ ). The sizes of the growing spherulites were followed by taking the digital images at appropriate intervals of time with an image processor (VCIC 2.0, homemade). The resolution of the measurement was  $1/30$  s.

For measurements of the melting points, the samples were annealed for 10 min at 100 °C (well above the melting point of pure PCL) and then rapidly quenched down to the crystallization temperature in a thermostat. After isothermal annealing for 12 h, the samples were brought to room temperature and the DSC measurements were performed immediately, with a Perkin-Elmer DSC7 using a heating rate of 10 K  $\text{min}^{-1}$ . The melting point was recorded at the peak temperature.

## Results and Discussion

Figure 1 shows the spherulites of PCL grown from the melt of pure material observed under crossed polarizers at 42 °C during the crystallization process. Figure 2 shows the spherulites of PCL grown from the melt of the blend of PCL/SAN (90/10) at 40 °C. It can

\* Abstract published in *Advance ACS Abstracts*, September 1, 1997.

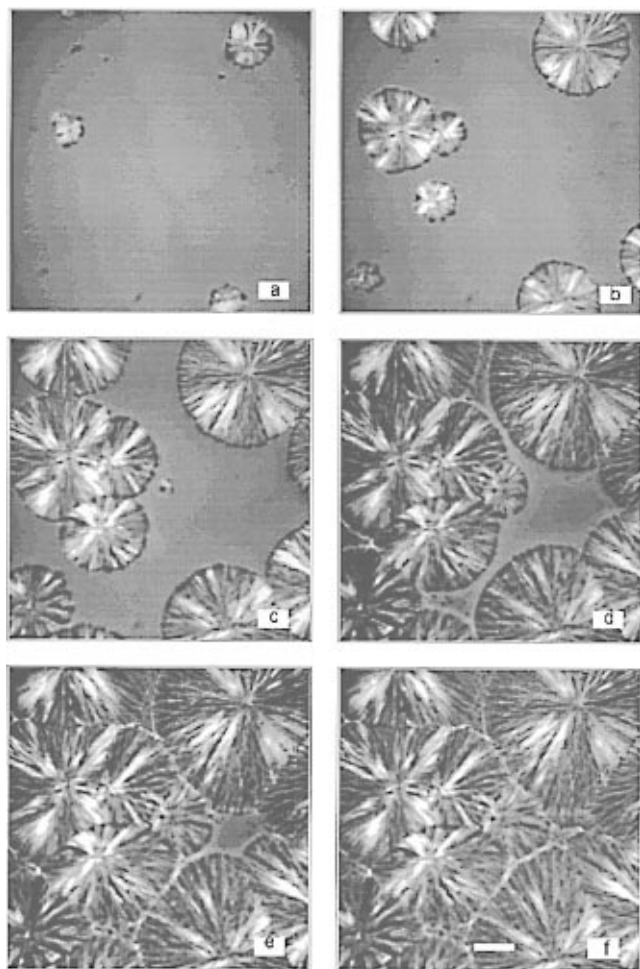


**Figure 1.** Polarized light micrographs of pure PCL crystallized at 42 °C from the melt: (a) 14 min; (b) 30 min; (c) 46 min; (d) 62 min; (e) 78 min; (f) 110 min. The white bar in (f) corresponds to 100  $\mu\text{m}$ .

be found that the spherulites of the blend exhibit not only a Maltese cross but also distinct extinction rings, which are named "ring-banded spherulites". The mechanism leading to this peculiar texture has not been clarified yet.<sup>23,26</sup> The formation of ring-banded spherulites may have some relationship with the crystallization kinetics of the blends, and this research is still not notified. In this paper, we are concerned only with the crystallization kinetics in mixtures of PCL and SAN.

In Figures 3 and 4 the radius of the spherulite is plotted against time at various crystallization temperatures for pure PCL and for the blend of PCL and SAN (90/10), respectively. The radii of the PCL spherulites increase linearly with time up to the impingement of the spherulites. From the slopes of these lines the isothermal radial growth rates,  $G$ , of the PCL spherulites for all  $T_c$  temperatures and compositions investigated were obtained. If the growth rates were affected by local changes of composition in the melt due to the rejection of noncrystallizable species from crystals, the growth rates would decrease with time in proportion to the concentration of noncrystallizable component at the growth front.<sup>31</sup> The constant  $G$  over the experiment range of time at the crystallization temperature infers that the concentration of SAN at the tips of radiating lamellae remains constant throughout the growth process. Thus, the radial diffusion of the rejected noncrystallizable component SAN is outstripped by the more rapid growth of the crystalline lamellae so that SAN is

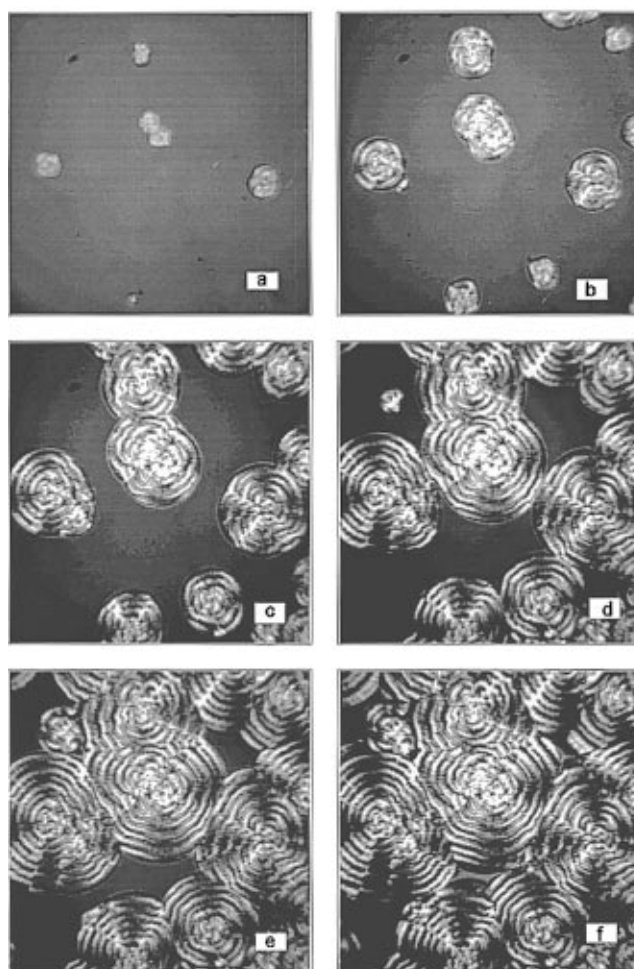


**Figure 2.** Polarized light micrographs of the blend of PCL/SAN (90/10) crystallized at 40 °C from the melt: (a) 7 min; (b) 13 min; (c) 21 min; (d) 29 min; (e) 37 min; (f) 41 min. The scale is the same as shown in Figure 1.

trapped between the growing lamellae.<sup>29</sup> Figure 5 shows a summary of all of the spherulitic isothermal growth rates measured, as a function of the crystallization temperature, for different blend ratios of PCL and SAN. It can be seen that the temperature dependence of growth rate for the mixtures is very similar to that for homopolymer PCL. However, with the increasing amount of SAN, the growth rate is somewhat slower. When compared with a pure polymer, the dilution of a crystallizable polymer should influence the free energy of nucleus formation and the transport process of the crystallizable polymer chain to the growing front of the crystal.

The experimental growth rate data were analyzed by a modified version of the phenomenological theory of nucleation of Turnbull and Fisher.<sup>6,8</sup> In this treatment, the rate of growth of the crystal,  $G$ , is governed by the work required to form a critical nucleus on the crystal surface,  $\Delta F^*$ , and by the energy required to transport segments across the solid-liquid interface,  $\Delta E$ . According to this theory

$$G = G_0 e^{-\Delta E/R(T-T_0)} e^{-\Delta F^*/k_b T} \quad (1)$$

where  $G_0$  is a constant that depends upon the regime of crystallization,  $R$  is the gas constant,  $T_0$  is the temperature at which motions necessary to transport segments across the liquid-solid interface cease,  $T$  is the temperature of crystallization, and  $k_b$  is the Boltz-

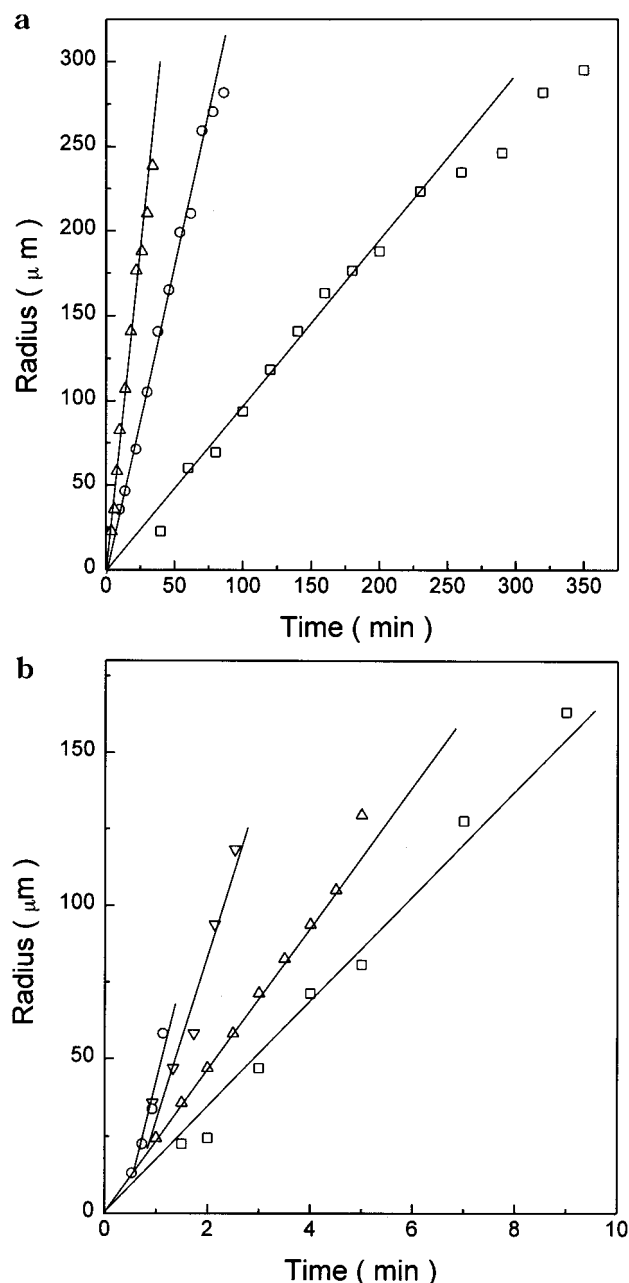


**Figure 3.** Variation in the spherulite radius with the crystallization time for pure PCL measured at different crystallization temperatures ( $^{\circ}\text{C}$ ): (a) ( $\square$ ) 45, ( $\circ$ ) 42, ( $\Delta$ ) 40; (b) ( $\square$ ) 37, ( $\Delta$ ) 35, ( $\nabla$ ) 33, ( $\circ$ ) 30.

mann constant. This equation produces the observed bell-shaped curve for the growth rate as a function of temperature. The growth rate is nucleation controlled at low undercooling and diffusion controlled at high undercooling.

For the compatible polymer mixtures of PCL and SAN, however, the process is somewhat more complex. The growth rate of PCL spherulite was reduced not only by the dilution of the crystallizable component but also by the chemical potential changes of the liquid phase due to specific interaction between the components. This interaction will alter the free energy necessary for forming a critical nucleus on the crystal surface and the mobility of both the crystallizable and noncrystallizable components. The PCL spherulitic growth rate in the mixtures will reflect the competition between the rate of transport of the crystallizable segments across the liquid–solid interface and the rate at which the amor-

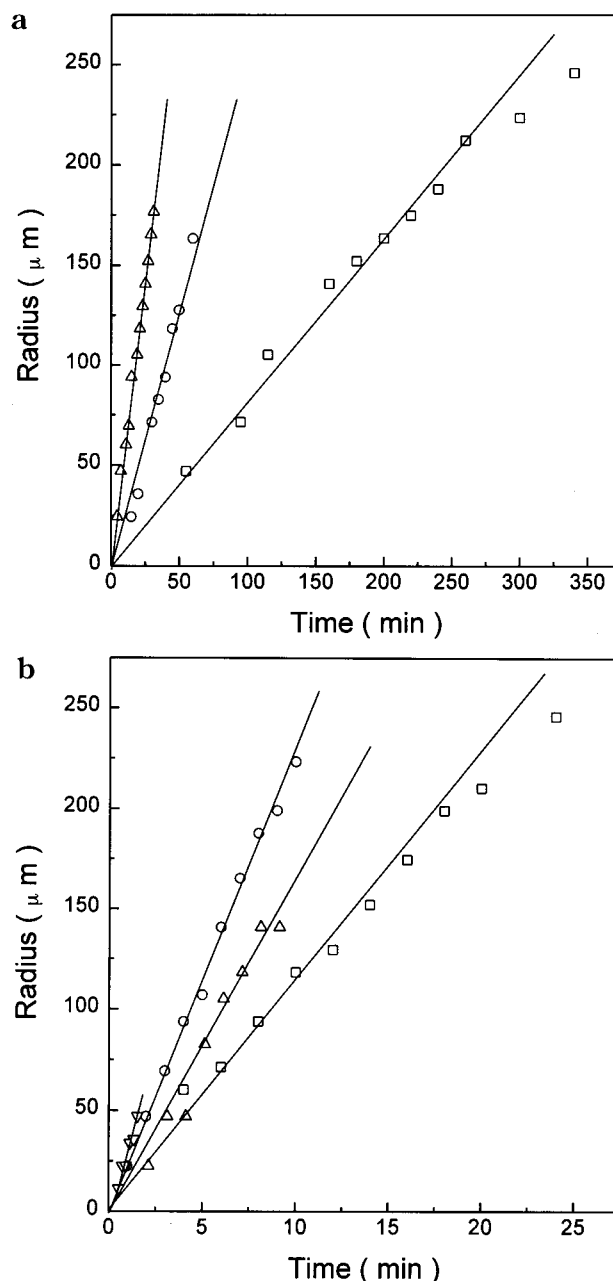


**Figure 4.** Variation in the spherulite radius with the crystallization time for the blend of PCL/SAN (90/10) measured at different crystallization temperatures ( $^{\circ}\text{C}$ ): (a) ( $\square$ ) 45, ( $\circ$ ) 42, ( $\Delta$ ) 40; (b) ( $\square$ ) 37, ( $\Delta$ ) 35, ( $\circ$ ) 33, ( $\nabla$ ) 30.

phous component can be removed from the growth front. This competition can be characterized by a length parameter  $\delta = D/G$  defined by Keith and Padden.<sup>1</sup>  $D$  is the diffusion coefficient of the noncrystallizable component in the crystallizing matrix, and  $G$  is the linear growth rate of the crystals. The parameter  $\delta$  represents the effective distance that the rejected noncrystallizable component may move during the time of crystallization. If  $\delta$  is comparable with the interlamellar distance, then the rejected material can reside between the lamellae. It has been proved that this is just the case for the PCL/SAN mixtures.<sup>29</sup> Therefore, the diffusion rate of the noncrystallizable component SAN may be neglected. A phenomenological equation describing the growth rate in the polymer mixtures has been given as

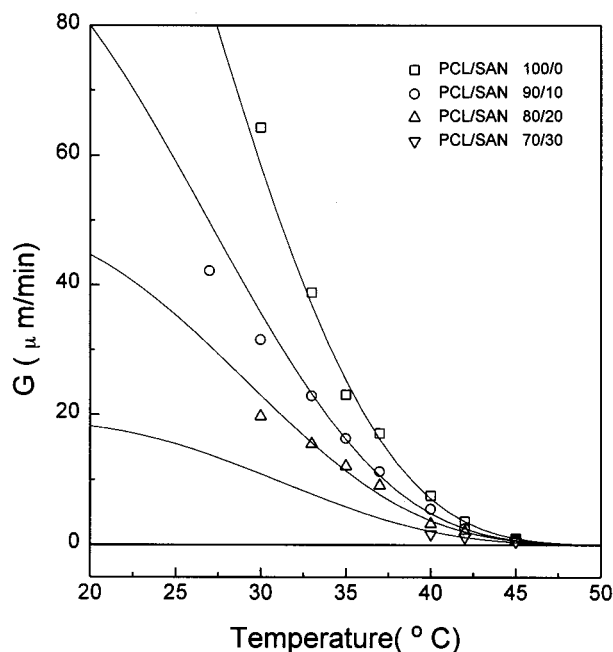


**Figure 5.** Variation in the spherulite growth rate  $G$  with the crystallization temperature shown for pure PCL and for PCL/SAN blends.

$$G_m = \phi_2 G_0 e^{-\Delta E/R(T-T_0)} e^{-\Delta F_m^*/k_b T_c} \quad (2)$$

where  $\phi_2$  is the volume fraction of the crystallizable component,  $G_0$  is a constant dependent on the regime of crystallization and is assumed equal to that of the pure semicrystalline polymer, and  $\Delta E$  is the energy necessary to achieve the transport of segments across the liquid–solid interface, which, due to the local nature of this term, is assumed to be the same as that of the pure semicrystalline polymer.<sup>16,32</sup> This idea has been put forth by Hoffman and co-workers that the molecular motions reflected in  $\Delta E$  and  $T_0'$  are not those associated with viscous flow and fluidity and no obvious decrease in  $\Delta E$  should occur upon dilution owing to a changing of the viscosity that results from addition of the amorphous polymer.<sup>8</sup>  $T_0'$  is similar to that found in the pure material except that  $T_0'$  must now be modified by the change in the glass transition temperature of the mixture,  $T_c$  is the crystallization temperature, and  $\Delta F_m^*$  is the free energy of critical nucleus formation on the crystal surface modified by the presence of the amorphous component.<sup>14</sup>  $T_0'$  is the value of  $T_0$  in the mixture and may be rewritten in terms of the glass transition temperature of the mixture,  $T_g$ , and a constant  $C$ . The constant,  $C$ , has been associated with the Williams, Landel, and Ferry universal constant  $C_2$ , which has a value of 51.6 °C.<sup>33</sup> In this study, the value of 105 °C is found to best fit all of the data.

Using a lattice treatment, Flory and later Mandelkern evaluated  $\Delta F_m^*$  for the case of semicrystalline polymers in the presence of a low molecular weight diluent.<sup>34,35</sup> Their treatment can be extended easily to the case of a polymer/polymer mixture such that

$$\Delta F_m^* = \frac{2b\sigma\sigma_e}{\Delta h_u f \left( 1 - \frac{T}{T_m^\circ} - \frac{RT\chi}{\Delta h_u f V_{1u}} (1 - \phi_2)^2 \right)} \quad (3)$$

where  $\Delta h_u$  is the heat of fusion per mole of monomer of the crystallizable component with volume fraction  $\phi_2$  at a temperature  $T$ ,  $T_m^\circ$  is the equilibrium melting point

**Table 1.** Parameters Used in Analysis<sup>a</sup>

	PCL	SAN
$\Delta E$ (J/mol)	17238.1	
$b$ (nm)	0.438	
$C$ (K)	105.0	
$\Delta h_u$ (J/m <sup>3</sup> )	$1.63 \times 10^8$	
$V_u$ (m <sup>3</sup> /mol)	$106.85 \times 10^{-6}$	$76.96 \times 10^{-6}$
$\chi$	-0.34	

<sup>a</sup> Data in the table are found in refs 1, 14, 29, 41, and 42.

of the pure material,  $V_{iu}$  is the molar volume of component  $i$ ,  $\chi$  is the Flory–Huggins interaction parameter,  $b$  is the thickness of the critical nucleus, and  $\sigma\sigma_e$  is the product of the lateral and fold surface free energies. The temperature dependence of  $\Delta h_u$  is embedded in the parameter  $f$ , which is given by

$$f = 2T/(T + T_m^\circ) \quad (4)$$

In addition to the assumptions inherent in the initial derivation of Flory,  $\chi$  is assumed independent of the temperature and composition.

By substituting the  $\Delta F_m^*$  into eq 2, the growth rate for the miscible PCL/SAN mixtures can be represented by the following equation:

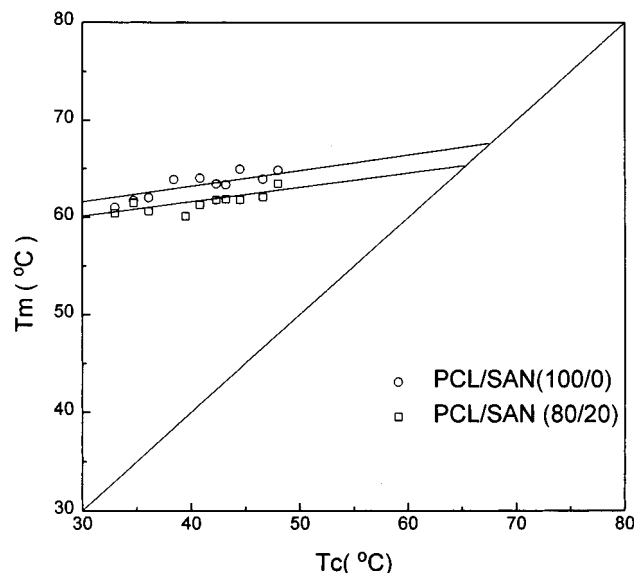
$$G_m = \phi_2 G_0 e^{-\Delta E/R(T-T_g+C)} \exp \left[ \frac{-2b\sigma\sigma_e}{k_b T \Delta h_u f \left( 1 - \frac{T}{T_m^\circ} - \frac{RTV_{2u}}{\Delta h_u f V_{1u}} \chi (1 - \phi_2)^2 \right)} \right] \quad (5)$$

The growth rate data for all the mixtures were analyzed according to eq 5. Use of this analysis requires values of  $\Delta E$ ,  $C$ ,  $b$ ,  $\Delta h_u$ ,  $V_{1u}$ ,  $V_{2u}$ , and  $\chi$ . The parameters used in these calculations are given in Table 1. The energy required to transport segments across the solid–liquid interface,  $\Delta E$ , was usually estimated by using the empirical relation of Williams, Landel, and Ferry (WLF) for the temperature dependence of the viscosity.<sup>1,14,33,36</sup> The magnitude of  $\Delta Z$  used in calculations for the mixtures was identical with that used in pure PCL, as discussed above.  $T_g$  for the mixtures was calculated from the Fox relationship.<sup>37</sup> It is reasonable to use this simple relationship, because experimental measurements on PCL blends confirm its validity.<sup>38</sup> The Lauritzen–Hoffman model was used to obtain the value of  $C$  according to the usual procedure.<sup>39</sup> The quantity  $\ln(G) + \Delta E/R(T - T_g + C)$  was plotted against  $1/(fT\Delta T)$ , while varying the value of  $C$  to maximize the correlation coefficient. An optimum fit value of  $C$  was found to be 105.0 for the mixtures of PCL and SAN. It has been reported that to fit growth rate with theory, values of  $C$  higher than 51.6 are needed. For example, Hoffman and Weeks reported a value of  $C = 130.0$  for nylon 6, and Alfonso et al. obtained  $C = 80.0$  for poly(ethylene oxide) (PEO).<sup>16,40</sup>

All other thermodynamic parameters such as  $\phi_2$ ,  $T_g$ , and  $T_m^\circ$  are listed in Table 2. The equilibrium melting points of pure PCL in the literature are not completely consistent due to the influence of supercooling, crystallization time (thickening effect), and molecular weight.<sup>16,29,30,41,43</sup>  $T_m^\circ$  of the pure PCL in our study was determined experimentally by using Hoffman–Weeks plots.<sup>44</sup> In the experiment,  $T_m$ , the measured nonequilibrium melting point, is plotted over  $T_c$  and extrapolated to the line where  $T_m = T_c$ . The intercept represents  $T_m^\circ$ . The data obtained for PCL are plotted in Figure 6. The value of  $T_m^\circ = 67.1$  °C in our study is

**Table 2.** Values of the Volume Fraction of PCL,  $T_g$  of the Mixtures, and the Equilibrium Melting Point  $T_m^\circ$  of the Mixtures

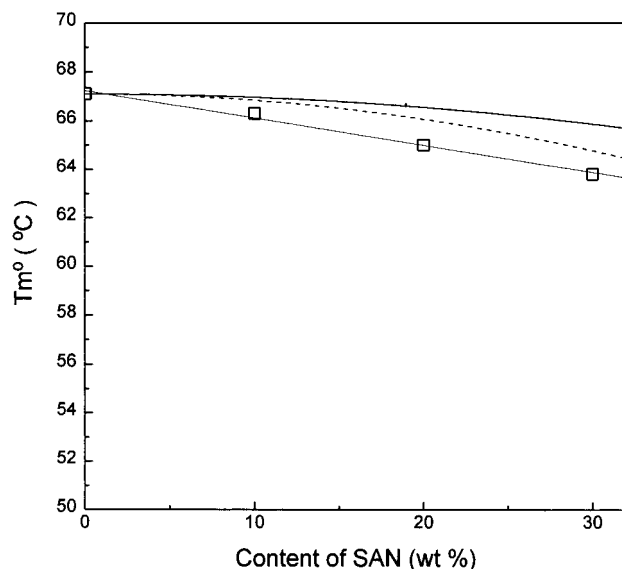
PCL/SAN	$\phi_2$	$T_g$ (°C)	$T_m^\circ$ (°C) <sup>a</sup>	$T_m^\circ$ (°C) <sup>b</sup>
100/0	1.000	-60.0	67.1	67.1
90/10	0.902	-50.3	66.8	66.3
80/20	0.803	-39.6	66.0	65.0
70/30	0.704	-27.9	64.7	63.8

<sup>a</sup> Obtained by using eq 6. <sup>b</sup> Obtained from experimental data.**Figure 6.** Hoffman-Weeks plots for the PCL/SAN blends.

a little higher than that obtained by Crescenzi et al. for PCL-700 using the diluent method and lower than these obtained by Phillips et al. and Kressler et al. for PCL-700 by the optical microscopy method and DSC method, respectively.<sup>30,41,43</sup> Usually, the values of  $T_m^\circ$  for the pure PCL should correspond to the values of  $T_m^\circ$  for a given molecular weight. The equilibrium melting points for the higher molecular weight were usually found to increase continuously.<sup>16</sup> The PCL in our study has a  $M_w$  of 22 000, which is lower than that of PCL-700. PCL-700 has a  $M_w$  of 40 000. In addition, when Crescenzi et al. obtained their value of 63 °C, they had not considered the effect of a diluent on the thickening process. Therefore, considering the influence of thickening effect and molecular weight, the degree of correspondence between these values is acceptable. The equilibrium melting points of the blends could be obtained by the same method, and their values versus SAN content are summarized in Table 2. The data obtained for the PCL/SAN (80/20) blend are plotted as an example in Figure 6. For the miscible polymer-polymer mixtures, as shown by Nishi and Wang, the Flory-Huggins theory predicts that the equilibrium melting point of the mixture,  $T_{m,eq}$ , will be lower than that of the pure material,  $T_m^\circ$ , such that<sup>15</sup>

$$\frac{1}{T_{m,eq}} = \frac{1}{T_m^\circ} - \frac{RV_{2u}}{\Delta h_u V_{1u}} \chi(1 - \phi_2)^2 \quad (6)$$

The equilibrium melting points of the mixtures calculated by using eq 6 are also listed in Table 2. The calculated and experimentally determined equilibrium melting points are shown in Figure 7, where it can be seen that the experimentally determined values are somewhat lower than the calculated ones. The reason for this might be experimental errors because in PCL/

**Figure 7.** Calculated equilibrium melting point of PCL blends with (---)  $\chi = -0.34$  and (—)  $\chi = -0.18$ . The symbol  $\square$  indicates the equilibrium melting points measured using Hoffman-Weeks plots.

SAN blends, secondary effects, causing deviations from linearity, become effective for crystallization temperatures lower than 45 °C, independent of the annealing time. Examples of secondary effects include recrystallization or chain mobility during the DSC run, leading to higher than actual  $T_m$  values.<sup>44</sup> It is also obvious that the range of crystallization temperatures required to obtain  $T_m^\circ$  is very narrow.<sup>41</sup> Neglecting this fact may lead to lower  $T_m^\circ$  values and to higher melting-point depressions in blends. Because of the very limited, useful range of crystallization temperatures, the somewhat involved extrapolation process and the expected small changes in the equilibrium melting points, we preferred to use the calculated equilibrium melting points of the blends.

The curves of growth rates of the mixtures, calculated with eq 5 from the experimental growth rates and the parameters in Tables 1 and 2 are presented in Figure 8. The experimental values of the growth rates fall well on the calculated curves. The preexponential factor  $G_0 = 134.7 \times 10^8 \mu\text{m}/\text{min}$  is obtained. The curves in Figure 5 are the same curves as shown in Figure 8. As can be seen more clearly from this plot, the experimental growth rates fall quite well on the calculated curves except for that at very high undercoolings (i.e., below 30 °C for the 90/10 blend and below 33 °C for 80/20 blend) where the experimental growth rates fall a little below theoretical curves of the growth rates. Whether this variation corresponds to the different growth rate regimes as discussed by Hoffmann et al. has not been known now, because the regime II crystallization has been proved for pure PCL and all (90/10) and (80/20) blends till temperatures fall to 32.5 °C.<sup>30,39</sup> Figure 8 shows that the maximum of the growth rates shifts to higher temperature with the increase of SAN content. This shift results from the changes of the glass transition temperatures ( $T_g$ ) and the melting points ( $T_m^\circ$ ) of the mixtures. In Figure 8, it is also shown that the growth rate of PCL spherulites is zero below the  $T_g$  of the PCL/SAN mixtures. From a thermodynamic viewpoint, specific interaction in the mixture leads to a slight depression in the equilibrium melting point and a change in the free energy for the formation of nuclei on the crystal surface. Another important parameter that

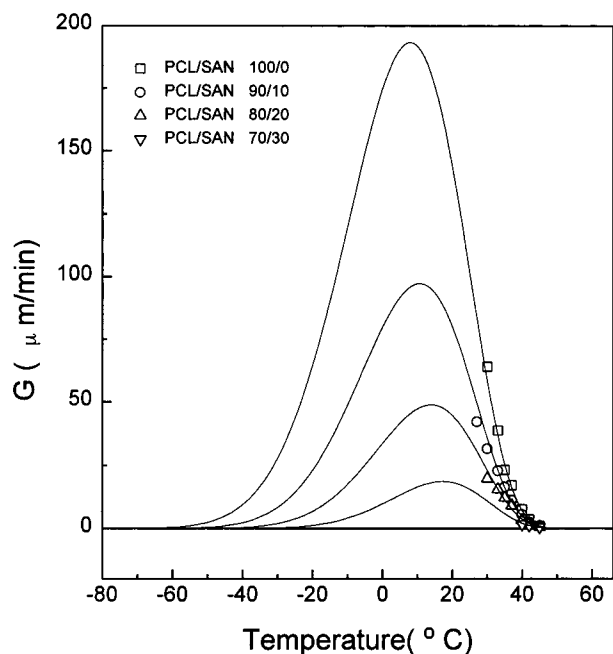


**Figure 8.** Curves of the spherulite growth rate  $G$  with the crystallization temperature calculated by using eq 5.

has significant influence on the overall mobility in the mixture is the glass transition temperature  $T_g$ . For PCL/SAN mixtures, most work has emphasized on the phase separation behavior and corresponding changes produced in the morphology.<sup>23–27</sup> Even for the kinetics of the crystallization process, the specific interactions in the mixture and the free energy for the formation of nuclei on the crystal surface have been pointed out for discussion.<sup>29,30</sup> However, the effect of  $T_g$  on the kinetics has been, more or less, ignored.

There are several obviously different values of the Flory–Huggins interaction parameter  $\chi$  for PCL/SAN blends obtained through experiments or theoretical calculation in the literature.<sup>25,29,30</sup> In the calculation described above, the value of  $-0.34$  for  $\chi$  from ref 29 was used and good results have been obtained. For comparison, another value of  $-0.18$  for  $\chi$  from ref 25 was incorporated, and the calculated data of growth rates of the mixtures are shown in Figure 9. As can be seen from these calculated data, significant agreement is observed although two different  $\chi$  were used. This could be the consequence of the lack of sensitivity of the melting point to the value of the interaction parameter that could easily be checked by introducing the value of  $-0.18$  in eq 6 and lead to an even lower decrease of the melting point with the concentration. The calculated result is also shown in Figure 7. The rather different values of interaction parameter do not affect very much the melting point  $T_m^\circ$  and therefore the degree of undercooling during crystallization. Furthermore, this may suggest that the free energy of critical nucleus formation on the crystal surface is not effectively modified by the presence of the amorphous component. The values of  $\sigma\sigma_e$  are displayed in Table 3 for the mixtures corresponding to two  $\chi$ , respectively. It can be seen that, with increasing SAN content, the surface free energies decrease slightly. Meanwhile, the change of  $\chi$  has not brought out a significant change of the surface free energies for the PCL/SAN mixtures of the same composition. Therefore, on one hand, it is thought that the interaction parameter  $\chi$  calculated by fitting the experimental data into eq 5 is questionable

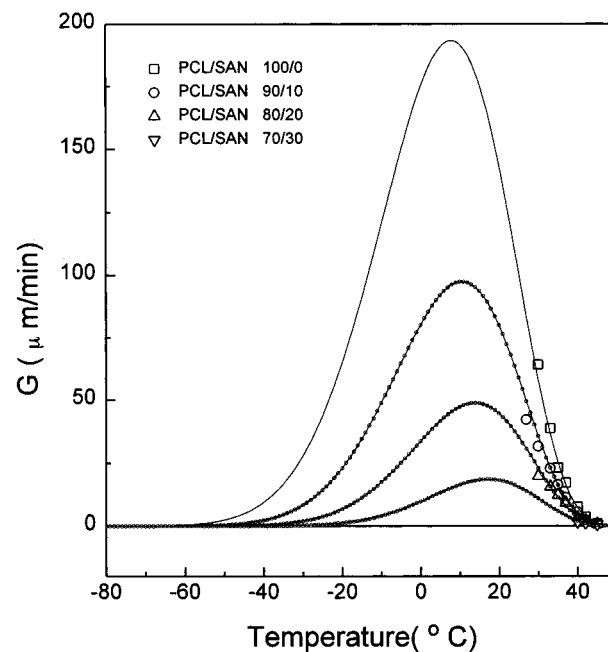


**Figure 9.** Curves of the spherulite growth rate  $G$  with the crystallization temperature calculated by using eq 5: (solid line)  $\chi = -0.34$ ; (○)  $\chi = -0.18$ .

**Table 3.** Values of  $\chi$  and  $\sigma\sigma_e$  of the PCL/SAN Mixtures

PCL/SAN	$\chi$	$\sigma\sigma_e$ ( $10^6$ J <sup>2</sup> /m <sup>4</sup> )	$\chi$	$\sigma\sigma_e$ ( $10^6$ J <sup>2</sup> /m <sup>4</sup> )
100/0		688.3		
90/10	$-0.34$	675.3	$-0.18$	675.1
80/20		648.2		647.1
70/30		631.0		629.1

and any agreement with other experimental techniques may be considered fortuitous.<sup>16,29</sup> On the other hand, the slight decrease of  $\sigma\sigma_e$  with composition and the nearly indistinguishable change with Flory–Huggins interaction parameter  $\chi$  may infer that the influence on the kinetics of crystallization is not obvious with the changes of surface free energies of the formation of nuclei on the crystal surface for the PCL/SAN mixtures.

On the contrary, with increasing SAN content, the parameter  $T_g$  of the mixtures has a significant increase, which can alter the transport term associated with the solid–liquid interface. The increase of  $T_g$  narrows the temperature range over which crystallization can occur, as is shown in Figure 5. For clearly demonstrating the effect of  $T_g$  on the kinetics, a slightly modified  $T_g$  by adding 2 °C was used and the calculated result is shown in Figure 10. The curve calculated using  $(T_g + 2)$  °C obviously falls below the experimental data. It is clear from this plot that  $T_g$  is a more important parameter that has a significant effect on the transport of the crystallizable segments across the liquid–solid interface. In fact, this transport term in eq 5 deals specifically with the local mobility of the segments, due to the interconnectivity of the polymer molecule, segments of the chain not crystallizing will be forced to undergo motions and, thus, will be affected by the overall mobility in the mixture. It is the overall mobility in the mixture that will be affected significantly by the  $T_g$  of the mixture. Therefore, it is considered that the influence of the overall mobility is predominant over the influence of the surface free energies on the PCL spherulitic growth rate in the mixtures. The specific interaction between the components of PCL and SAN in the mixtures will slightly alter the free energy necessary to form a critical nucleus on the crystal

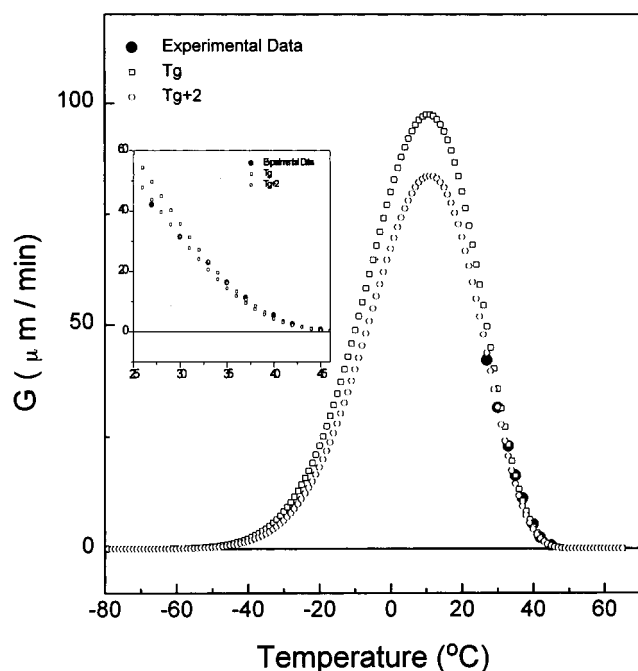


**Figure 10.** Curves of the spherulite growth rate  $G$  with the crystallization temperature for the blend of PCL/SAN (90/10) calculated by using eq 5 for indicating the influence of  $T_g$  on the growth rate.

surface and significantly alter the mobility of both the crystallizable and noncrystallizable components through the higher  $T_g$  of the amorphous component of SAN involved. This problem has been treated in a different way in the literature, in which it was concluded that the influence of mobility is predominant over the influence of the surface free energy related to some conditions including crystallization temperature, composition of amorphous component, or the diffusion of amorphous component, thus leading to a decrease of the spherulitic growth rate.<sup>1,16,28,30</sup>

## Conclusions

A study on the crystallization kinetics of PCL/SAN mixtures has been performed over a wide range of crystallization temperatures and several compositions. A phenomenological equation has been used to analyze the experimental data and has been found to describe the observed growth rates quite well. The influences of the surface free energy necessary to form a critical nucleus on the crystal surface and of the mobility of both the crystallizable and noncrystallizable components, that is, the overall mobility on the PCL spherulitic growth rate in the mixtures, have been discussed. The experimental findings show that the influence of the overall mobility is predominant over the influence of the surface free energy, indicating that the glass transition temperature of the mixtures should be of main importance. In addition it has been found that evaluation of the Flory–Huggins interaction parameter through fitting the experimental data into the phenomenological equation is questionable.

**Acknowledgment.** This research was supported by “National Basic Research Project-Macromolecular Condensed State” Foundation of China.

## References and Notes

- (1) Keith, H. D.; Padden, F. J. *J. Appl. Phys.* **1964**, *35*, 1270 and 1286.
- (2) Hoffman, J. D.; Frolen, L. J.; Ross, G. S.; Lauritzen, J. I., Jr. *J. Res. Natl. Bur. Std.* **1975**, *79A*, 671.
- (3) Lovinger, A.; Davis, D. D.; Padden, F. J., Jr. *Polymer* **1985**, *26*, 1595.
- (4) Clark, E. J.; Hoffman, J. D. *Macromolecules* **1984**, *17*, 878.
- (5) Cheng, S. Z.; Chen, J.; Janimak, J. J. *Polymer* **1990**, *31*, 1018.
- (6) Turnbull, D.; Fisher, J. C. *J. Chem. Phys.* **1949**, *17*, 71.
- (7) Hoffman, J. D.; Lauritzen, J. I., Jr. *J. Res. Natl. Bur. Std.* **1961**, *65A*, 297.
- (8) Lauritzen, J. I., Jr.; Hoffman, J. D. *J. Appl. Phys.* **1973**, *44*, 4340.
- (9) Hoffman, J. D. *Polymer* **1982**, *23*, 656.
- (10) Hoffman, J. D. *Polymer* **1983**, *24*, 3.
- (11) Hoffman, J. D. *Polymer* **1985**, *26*, 803.
- (12) Hoffman, J. D. *Polymer* **1985**, *26*, 1763.
- (13) Hoffman, J. D.; Miller, R. L. *Macromolecules* **1988**, *21*, 3038.
- (14) Ong, C. J.; Price, F. P. *J. Polym. Sci., Polym. Symp.* **1978**, *63*, 59.
- (15) Nishi, T.; Wang, T. T. *Macromolecules* **1975**, *8*, 909.
- (16) Alfonso, G. C.; Russell, T. P. *Macromolecules* **1986**, *19*, 1143.
- (17) Marand, H.; Collins, M. *Polym. Prepr. (Am. Chem. Soc., Div. Polym. Chem.)* **1990**, *31*, 552.
- (18) Runt, J.; Miley, D. M.; Zhang, X.; Galiagher, K. P.; McFeaters, K.; Fishbarn, J. *Macromolecules* **1992**, *25*, 1929.
- (19) De Juana, R.; Cortazar, M. *Macromolecules* **1993**, *26*, 1170.
- (20) Saito, H.; Okada, T.; Hamane, T.; Inoue, T. *Macromolecules* **1991**, *24*, 4446.
- (21) Okada, T.; Saito, H.; Inoue, T. *Polymer* **1994**, *35*, 5699.
- (22) Chiu, S. C.; Smith, T. G. *J. Appl. Polym. Sci.* **1984**, *29*, 1797.
- (23) Schulze, K.; Kressler, J.; Kammer, H. W. *Polymer* **1993**, *34*, 3704.
- (24) Svoboda, P.; Kressler, J.; Chiba, T.; Inoue, T.; Kammer, H. W. *Macromolecules* **1994**, *27*, 1154.
- (25) Kressler, J.; Kammer, H. W. *Polym. Bull.* **1988**, *19*, 283.
- (26) Kummerlowe, C.; Kammer, H. W. *Polym. Networks Blends* **1995**, *5* (3), 131.
- (27) Janarthanan, V.; Kressler, J.; Karasz, F. E.; Macknight, W. J. *J. Polym. Sci., Polym. Phys.* **1993**, *31*, 1013.
- (28) Kressler, J.; Svoboda, P.; Inoue, T. *Polym. Prepr. (Am. Chem. Soc., Div. Polym. Chem.)* **1992**, *33* (2), 612.
- (29) Li, W.; Yan, R. J.; Jiang, B. Z. *J. Macromol. Sci., Phys.* **1992**, *B31* (2), 227.
- (30) Kressler, J.; Svoboda, P.; Inoue, T. *Polymer* **1993**, *34*, 3225.
- (31) Tanaka, H.; Nishi, T. *Phys. Rev. A* **1989**, *39*, 783.
- (32) Wang, T. T.; Nishi, T. *Macromolecules* **1977**, *10*, 421.
- (33) Williams, M. C.; Landel, R. F.; Ferry, J. D. *J. Am. Chem. Soc.* **1955**, *77*, 3701.
- (34) Flory, P. J. *J. Chem. Phys.* **1949**, *17*, 223.
- (35) Mandelkern, L. *J. Appl. Phys.* **1955**, *26*, 443.
- (36) Calahorra, E.; Cortazar, M.; Guzman, G. M. *Polymer* **1982**, *23*, 1322.
- (37) Fox, T. G. *Bull. Am. Phys. Soc.* **1956**, *1*, 123.
- (38) Koleske, J.; Lundberg, R. *J. Polym. Sci., Polym. Phys. Ed.* **1969**, *7*, 795.
- (39) Hoffman, J. D.; Davis, G. T.; Lauritzen, J. I., Jr. In *Treatise on Solid State Chemistry*; Hannay, N. B., Ed.; Plenum Press: New York, 1976; Vol. 3, Chapter 7.
- (40) Hoffmann, J. D.; Weeks, J. J. *J. Chem. Phys.* **1962**, *37*, 1723.
- (41) Phillips, P. J.; Rensch, G. J.; Taylor, K. D. *J. Polym. Sci., Polym. Phys.* **1987**, *25*, 1725.
- (42) Van Krevelen, D. W. *Properties of Polymers*; Elsevier: Amsterdam, 1976.
- (43) Crescenzi, V.; Mancini, G.; Calzolari, G.; Borri, C. *Eur. Polym. J.* **1972**, *8*, 449.
- (44) Hoffman, J. D.; Weeks, J. J. *J. Res. Natl. Bur. Std.* **1962**, *66A*, 13.

MA961458H